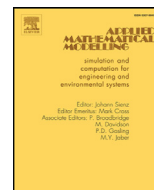




Contents lists available at ScienceDirect

Applied Mathematical Modelling

journal homepage: www.elsevier.com/locate/apm

Two-grid variational multiscale method with bubble stabilization for convection diffusion equation

Zhifeng Weng^a, Jerry Zhijian Yang^{a,b}, Xiliang Lu^{a,b,*}

^a School of Mathematics and Statistics, Wuhan University, Wuhan 430072, PR China

^b Computational Science Hubei Key Laboratory, Wuhan University, Wuhan, 430072, PR China

ARTICLE INFO

Article history:

Received 20 March 2014

Revised 4 May 2015

Accepted 17 June 2015

Available online xxx

Keywords:

Convection diffusion equation

Variational multiscale method

Two-grid method

Local Gauss integrations

Bubble functions

ABSTRACT

A two-grid variational multiscale (VMS) method based on two local Gauss integrations for the convection dominated nonlinear convection diffusion equation is investigated. This method combines the two-grid strategy with the variational multiscale method which chooses polynomial bubble functions as subgrid scale. Two local Gauss integrations are applied to replace the projection operator without adding any extra storage. Moreover, the error estimates for the algorithms of the two-grid method are obtained. Numerical examples validate the theoretical results of the presented methods.

© 2015 Elsevier Inc. All rights reserved.

1. Introduction

The convection diffusion equations describe a lot of physical phenomenons in computational fluid dynamics such as chemical reaction processes, heat conduction, nuclear reactors, population dynamics, just to name a few. The governing equations are often with a nonlinear source or sink term. In this work we consider the following stationary nonlinear convection diffusion equations:

$$\alpha \cdot \nabla u - \varepsilon \Delta u = f(u), \quad \text{in } \Omega, \quad (1)$$

$$u = 0, \quad \text{on } \partial\Omega, \quad (2)$$

where $\Omega \subset \mathbb{R}^2$ is a bounded domain with C^2 boundary $\partial\Omega$. The constant ε is the diffusion coefficient and α is either a constant vector or a divergence free velocity field. The nonlinear reaction terms $f(u)$ appear usually in the form of products and rational functions of concentrations, or exponential functions of the temperature, expressed by the Arrhenius law in chemical engineering.

When $\varepsilon \ll 1$, Eq. (1)–(2) is a convection dominated problem. The standard continuous piecewise linear finite element method may produce a large non-physical oscillations to the approximate solutions, unless the mesh size is small enough with respect to the diffusion coefficient. In order to overcome the numerical instabilities, people introduce different stabilization methods, such as, the Galerkin least square (GLS) method [1,2], stream upwind Petrov Galerkin (SUPG) method [3,4], the residual-free bubbles (RFB) method [5,6], the local projection stabilization [7,8] and etc. for linear convection dominated problems. For nonlinear convection dominated problems, Markus Bause in [9] provided SUPG stabilized higher-order finite element approximations of

* Corresponding author.

E-mail addresses: zfweng@whu.edu.cn (Z. Weng), zjyang.math@whu.edu.cn (J.Z. Yang), xllv.math@whu.edu.cn (X. Lu).

convection diffusion reactions models with nonlinear reaction mechanisms. Markus et al. [10,11] analyzed the numerical performance properties of higher order finite element approaches along with SUPG and additional shock-capturing stabilization for nonlinear convection dominated problem. Yücel et al. [12] studied convection diffusion reaction models with nonlinear reaction mechanisms by using the discontinuous Galerkin method and the upwind symmetric interior penalty Galerkin (SIPG) method.

However, the SUPG methods have some drawbacks in application: it brings in additional nonphysical coupling term and hence unphysical oscillations near the boundary; and the second order derivative is needed for the high order finite element approximations. To overcome those drawbacks of SUPG methods, alternative some stabilization methods have been reformulated in the framework of the variational multiscale method. Hughes [13] proposed the variational multiscale method (VMS) to overcome spurious oscillations in solutions which is caused by the multiscale structure of the problem. The VMS method decomposes the solution into large scale and small scale such that one can obtain a coupled system of two sub-problems for the different scales. In such way one can obtain a stabilized formulation. There are different ways to define the large scale problem in the variational multiscale method, for example, projection into appropriate subspaces is applied in Hughes et al. [14,15], Guermond [16], Layton [17,18] and Zheng et al. [19]. Especially, Song et al. [20] proposed a variational multiscale method based on polynomial bubble functions as subgrid scale for linear convection dominated convection diffusion equation. Similar as the work of Song et al. [20], we extend this method to solve the nonlinear convection diffusion problem. More precisely, we add an eddy viscosity stabilization which chooses a bubble function as subgrid scale, and the projection operator is reformulated by the local Gaussian quadrature. It keeps the same efficiency without adding any extra storage compared with common VMS in [21].

To increase the efficiency of a numerical method, an alternative idea is the two-grid method. The two-grid discretization strategy is to compute the nonlinear equation on a coarse mesh, then to solve a linearized system (at the solution from coarse mesh) on a fine mesh. The two-grid method can be found in the works of Xu [22,23], Chen et al. [24], He et al. [25–27], Zhang and He [28], Shang [29], Huang et al. [30], Weng et al. [31] and etc.

In this paper we combine the two-grid method with the variational multiscale method for solving the two-dimensional steady convection diffusion problem based on the locally stabilized method with Gaussian quadrature rule. The remainder of this paper is organized as follows. In Section 2, a variational multiscale finite element method is introduced. The two-grid method is given in Sections 3. In Section 4, numerical experiments are given to validate the theoretical results.

The standard Sobolev space $W^{m,p}(\Omega)$ is equipped with a norm $\|\cdot\|_{m,p}$. For $p = 2$, let $H^m(\Omega) = W^{m,2}(\Omega)$ and write $\|\cdot\|_m = \|\cdot\|_{m,2}$ and $\|\cdot\| = \|\cdot\|_{0,2}$. We use the constant C or c to denote a generic positive constant whose value may change from place to place, but remains independent of the mesh parameter and ε .

2. Variational multiscale finite element method

2.1. Variational formulation of the convection–diffusion problem

Define bilinear forms $a(\cdot, \cdot)$, $b(\cdot, \cdot)$ and $B(\cdot, \cdot)$ on $H_0^1(\Omega) \times H_0^1(\Omega)$ by

$$a(u, v) = \varepsilon(\nabla u, \nabla v), \quad b(u, v) = (\alpha \cdot \nabla u, v), \quad B(u, v) = a(u, v) + b(u, v).$$

Then the variational formulation of problem (1)–(2) reads: find $u \in H_0^1(\Omega)$ such that

$$B(u, v) = (f(u), v), \quad \forall v \in H_0^1(\Omega). \quad (3)$$

We assume the nonlinear term f is a locally Lipschitz, monotone function and is bounded up to second order derivative, i.e. for any $t, t_1, t_2 \geq 0$, $t, t_1, t_2 \in \mathbb{R}$ the following conditions

$$\begin{aligned} \|f(t_1) - f(t_2)\| &\leq L\|t_1 - t_2\|, \quad L > 0 \\ f &\in C^2(\mathbb{R}), \quad f'(t) \leq 0, \quad |f(t)| + |f''(t)| \leq C \end{aligned} \quad (4)$$

So that (3) admits a unique solution $u \in H_0^1(\Omega)$ (c.f. [16]).

2.2. Variational multiscale finite element method based on two local Gauss integrations

Let $M_h \subseteq H_0^1(\Omega)$ be a standard piecewise polynomial finite element defined on Ω and let u_h be the finite element approximation solution of problem (3), and satisfy

$$B(u_h, v_h) = (f(u_h), v_h) \quad \forall v_h \in M_h. \quad (5)$$

It is known that the formulation (5) lacks coercivity when $\varepsilon \ll |\alpha|$, unless the mesh size h is small enough with respect to the diffusion coefficient ε . The common variational multiscale methods in [21] to stabilize (5) is as follows: let \mathbf{L}_h be a vector valued finite element subspace of $[L^2(\Omega)]^2$, to find $u_h \in M_h$, $\mathbf{P}_h \in \mathbf{L}_h$ satisfying

$$\begin{aligned} B(u_h, v_h) + (v \nabla u_h, \nabla v_h) - (v \mathbf{P}_h, \nabla v_h) &= (f(u_h), v_h), \quad \forall v_h \in M_h, \\ (\mathbf{P}_h - \nabla u_h, \mathbf{I}_h) &= 0, \quad \forall \mathbf{I}_h \in \mathbf{L}_h. \end{aligned} \quad (6)$$

The second equation in (6) implies that \mathbf{P}_h is the L^2 -orthogonal projection of ∇u_h into \mathbf{L}_h . The space \mathbf{L}_h contains the information of the coarse scale, and the stabilization parameter v acts only on the fine scale. The choice of v is discussed in [21]. The constant

ν should be chosen as the scale of $O(h)$ in order to stabilize the convective term appropriately. There are two common choices for $\mathbf{L}_{\tilde{h}}$, e.g., $\mathbf{L}_{\tilde{h}}$ can be a finite element space on a coarse mesh [21], or a lower order finite element on the same mesh. In this article we will use the later one.

Now we give the finite element discretization. Let T_h be the quasi-uniform triangulations of the domain Ω with the mesh size $h = \max\{\text{diam}(K) : K \in T_h\}$. The finite element spaces are defined by

$$\begin{aligned} M_1 &= \{u_h \in C(\Omega) \mid u_h|_K \in P_1(K), \forall K \in T_h\}, \\ M_b &= \{u_h \in C(\Omega) \mid u_h|_K \in B(K), \forall K \in T_h\}, \\ M_h^b &= \{v_h \in C(\Omega) \mid v_h|_K \in P_1(K) \oplus B(K), \forall K \in T_h\}, \end{aligned}$$

where $P_1(K)$ is the space of first-order polynomials on K and $B(K)$ denotes the bubble functions on K as follows:

$$B(K) = \{u_h \in C(K) \mid u_h \in \text{Span}\{\lambda^0 \lambda^1 \lambda^2\}, \quad \forall K \in T_h\},$$

where λ^i are area coordinates on K , $i = 0, 1, 2$.

We will also need the piecewise constant vector space

$$\mathbf{R}_0 = \{\mathbf{V}_h \in [L^2(\Omega)]^2 \mid \mathbf{V}_h|_K \in [P_0(K)]^2, \forall K \in T_h\},$$

where $P_0(K)$ is piecewise constant on K .

We choose (M_h^b, \mathbf{R}_0) as the pair $(M_h, \mathbf{L}_{\tilde{h}})$ in the common variational multiscale schemes (6). Therefore the discrete equation reads: find $u_h \in M_h^b, \mathbf{P}_{\tilde{h}} \in \mathbf{R}_0$ satisfying

$$\begin{aligned} B(u_h, v_h) + (\nu \nabla u_h, \nabla v_h) - (\nu \mathbf{P}_{\tilde{h}}, \nabla v_h) &= (f(u_h), v_h), \quad \forall v_h \in M_h^b, \\ (\mathbf{P}_{\tilde{h}} - \nabla u_h, \mathbf{I}_{\tilde{h}}) &= 0, \quad \forall \mathbf{I}_{\tilde{h}} \in \mathbf{R}_0. \end{aligned} \tag{7}$$

It is noted that the extra storage is required by (7) due to the two additional dependent variables in $\mathbf{P}_{\tilde{h}}$ are introduced. In order to avoid the extra storage, we define the orthogonal projection operator $\Pi: [L^2(\Omega)]^2 \rightarrow \mathbf{R}_0$ as follows [32]:

$$\|\Pi \mathbf{g}\| \leq C \|\mathbf{g}\|, \quad \forall \mathbf{g} \in [L^2(\Omega)]^2, \tag{8}$$

$$(\mathbf{g} - \Pi \mathbf{g}, \mathbf{g}_h) = 0, \quad \forall \mathbf{g} \in [L^2(\Omega)]^2, \mathbf{g}_h \in \mathbf{R}_0, \tag{9}$$

$$\|\mathbf{g} - \Pi \mathbf{g}\| \leq Ch \|\mathbf{g}\|_1, \quad \forall \mathbf{g} \in [H^1(\Omega)]^2. \tag{10}$$

Then, with the orthogonal property, the stabilized form $G(\cdot, \cdot)$ can be rewritten by

$$G(u_h, v_h) = \nu (\nabla u_h, \nabla v_h) - \nu (\Pi \nabla u_h, \Pi \nabla v_h).$$

Therefore, the equivalent formulation of (7) (c.f. [20]) can be casted in the framework of VMS method as follows :

$$B(u_h, v_h) + \nu (\nabla u_h, \nabla v_h) - \nu (\Pi \nabla u_h, \Pi \nabla v_h) = (f(u_h), v_h). \tag{11}$$

Under the assumption (4) of f , the existence of a unique solution to (11) can be found in [16].

By careful computation, we find the stabilization term $G(u_h, v_h)$ can be explicitly expressed as the difference between two local Gauss integrations at each element:

$$G(u_h, v_h) = \nu \sum_{K \in T_h} \left(\int_{K,k} \nabla u_h \nabla v_h \, d\Omega - \int_{K,1} \nabla u_h \nabla v_h \, d\Omega \right), \quad \forall u_h, v_h \in M_h^b,$$

where $\int_{K,i} g(x) dx$ indicates an approximation Gauss integral over K which is exact for polynomials of degree i , $i = 1, k (k \geq 2)$. $\int_{K,1} g(x) dx$ is equivalent to 1 point Gauss integration over K . And ν is the stabilization parameter.

Obviously, the formulation (11) introduces no additional dependent variables. So this formulation is more effective than the formulation (7). The numerical tests in later section will also verify it.

Moreover, in order to obtain the error estimates, we can introduce interpolation operator $\Pi_h: H^2(\Omega) \cap H_0^1(\Omega) \rightarrow M_h^b$, which satisfies the following approximation properties in [34]:

$$\|\Pi_h v\|_1 \leq C \|v\|_1, \quad \forall v \in H_0^1(\Omega), \tag{12}$$

$$\|v - \Pi_h v\| + h \|v - \Pi_h v\|_1 \leq Ch^2 \|v\|_2, \quad \forall v \in H_0^1(\Omega) \cap H^2(\Omega). \tag{13}$$

Next, we will give the following priori error estimates.

Theorem 2.1. Let $u \in H^2(\Omega) \cap H_0^1(\Omega)$ and $u_h \in M_h^b$ be the solution of (3) and (11), respectively. Then we have the the following error estimate:

$$\|u - u_h\|_1 \leq C \left(1 + \frac{h}{\varepsilon} + \sqrt{\frac{\nu}{\varepsilon}} \right) h \|u\|_2. \tag{14}$$

Proof. Using Taylor expansion, we can get

$$f(u) - f(u_h) = f'(\bar{u}_h)(u - u_h),$$

where \bar{u}_h is some value between u and u_h . Subtracting (3) from (11) we obtain

$$B(u - u_h, v_h) + G(u - u_h, v_h) = G(u, v_h) + (f'(\bar{u}_h)(u - u_h), v_h). \tag{15}$$

Set $\eta = u - \Pi_h u$ and $\phi_h = u_h - \Pi_h u$, then $u - u_h = \eta - \phi_h$. Rearranging the terms of (15), choosing $v_h = \phi_h \in M_h^b$, we have

$$\begin{aligned} &\varepsilon(\nabla\phi_h, \nabla\phi_h) + G(\phi_h, \phi_h) \\ &= \varepsilon(\nabla\eta, \nabla\phi_h) + (\alpha \cdot \nabla\eta, \phi_h) + G(\eta, \phi_h) \\ &\quad - G(u, \phi_h) + f'(\bar{u}_h)(\phi_h - \eta, \phi_h). \end{aligned} \tag{16}$$

By Cauchy–Schwarz inequality and Young’s inequality and the Sobolev imbedding theorem and from (8) and (10), we obtain

$$\varepsilon(\nabla\eta, \nabla\phi_h) \leq \varepsilon\|\eta\|_1\|\phi_h\|_1 \leq \varepsilon\|\eta\|_1^2 + \frac{\varepsilon}{4}\|\nabla\phi_h\|^2,$$

$$(\alpha \cdot \nabla\eta, \phi_h) = -(\eta, \alpha \cdot \nabla\phi_h) \leq \frac{C}{\varepsilon}\|\eta\|^2 + \frac{\varepsilon}{4}\|\nabla\phi_h\|^2,$$

$$\begin{aligned} G(\eta, \phi_h) &= \nu((I - \Pi)\nabla\eta, (I - \Pi)\nabla\phi_h) \\ &\leq \nu\|(I - \Pi)\nabla\eta\|\|(I - \Pi)\nabla\phi_h\| \\ &\leq C\nu\|\eta\|_1^2 + \frac{\nu}{4}\|(I - \Pi)\nabla\phi_h\|^2, \end{aligned}$$

$$\begin{aligned} G(u, \phi_h) &= \nu((I - \Pi)\nabla u, (I - \Pi)\nabla\phi_h) \\ &\leq \nu\|(I - \Pi)\nabla u\|\|(I - \Pi)\nabla\phi_h\| \\ &\leq C\nu h^2\|u\|_2^2 + \frac{\nu}{4}\|(I - \Pi)\nabla\phi_h\|^2, \end{aligned}$$

$$\begin{aligned} f'(\bar{u}_h)(\phi_h - \eta, \phi_h) &= f'(\bar{u}_h)((\phi_h, \phi_h) - (\eta, \phi_h)) \\ &\leq C\|\eta\|\|\phi_h\| + f'(\bar{u}_h)\|\phi_h\|^2 \\ &\leq \frac{\varepsilon}{4}\|\nabla\phi_h\|^2 + \frac{C}{\varepsilon}\|\eta\|^2. \end{aligned}$$

Then we rewrite (16) as follows:

$$\begin{aligned} &\varepsilon(\nabla\phi_h, \nabla\phi_h) + G(\phi_h, \phi_h) \\ &= \varepsilon\|\nabla\phi_h\|^2 + \nu\|(I - \Pi)\nabla\phi_h\|^2 \\ &\leq \frac{3\varepsilon}{4}\|\nabla\phi_h\|^2 + \frac{\nu}{2}\|(I - \Pi)\nabla\phi_h\|^2 + C(\varepsilon + \nu)\|\eta\|_1^2 + \frac{C}{\varepsilon}\|\eta\|^2 + C\nu h^2\|u\|_2^2. \end{aligned} \tag{17}$$

From (17), we have

$$\varepsilon\|\phi_h\|_1^2 \leq C(\varepsilon + \nu)\|\eta\|_1^2 + \frac{C}{\varepsilon}\|\eta\|^2 + C\nu h^2\|u\|_2^2. \tag{18}$$

From (13) and (18), then by the triangle inequality, we can get:

$$\begin{aligned} &\varepsilon\|u - u_h\|_1^2 \\ &\leq \varepsilon(\|\eta\|_1^2 + \|\phi_h\|_1^2) \\ &\leq C(\varepsilon + \nu)\|\eta\|_1^2 + \frac{C}{\varepsilon}\|\eta\|^2 + C\nu h^2\|u\|_2^2 \\ &\leq C\left(\varepsilon + \frac{h^2}{\varepsilon} + \nu\right)h^2\|u\|_2^2. \end{aligned} \tag{19}$$

Finally, we can obtain the result of (14). \square

Then we will give the L^2 -error estimate for the finite element approximation solution u_h of (11) to the exact solution u of (3), one has the following result.

Theorem 2.2. Suppose that $u \in H^2(\Omega) \cap H_0^1(\Omega)$ and $u_h \in M_h^b$ be the solution (3) and (11), respectively. Then we can obtain a priori estimate as follows:

$$\|u - u_h\| \leq C\left(1 + \frac{h}{\varepsilon} + \sqrt{\frac{\nu}{\varepsilon}}\right)\left(1 + \frac{h}{\varepsilon} + \frac{\nu}{\varepsilon}\right)h^2\|u\|_2 + C\frac{1}{\varepsilon^2}\left(\varepsilon + \frac{h^2}{\varepsilon} + \nu\right)h^2\|u\|_2^2. \tag{20}$$

Proof. By Taylor expansion, we obtain

$$f(u) - f(u_h) = f'(u_h)(u - u_h) + f''(\phi_1)(u - u_h)^2, \tag{21}$$

$$f'(u) - f'(u_h) = f''(\phi_2)(u - u_h), \tag{22}$$

where ϕ_1 and ϕ_2 are some value between u and u_h . Let $\Phi \in H_0^1(\Omega)$ be the solution of the auxiliary problem

$$\varepsilon(\nabla v, \nabla \Phi) - (v, \alpha \cdot \nabla \Phi) - (f'(u)v, \Phi) = (v, u - u_h), \quad \forall v \in H_0^1(\Omega), \tag{23}$$

then we have [33]

$$\varepsilon \|\Phi\|_2 \leq c \|u - u_h\|. \tag{24}$$

Choosing $v = u - u_h$ in (23) and using Cauchy–Schwarz inequality, we can get

$$\begin{aligned} \|u - u_h\|_0^2 &= \varepsilon(\nabla \Phi, \nabla(u - u_h)) - (\alpha \cdot \nabla \Phi, u - u_h) - (f'(u)(u - u_h), \Phi) \\ &= \varepsilon(\nabla u - \nabla u_h, \nabla \Phi) + (\alpha \cdot (\nabla u - \nabla u_h), \Phi) - (f'(u)(u - u_h), \Phi) \\ &= \varepsilon(\nabla u - \nabla u_h, \nabla \Phi - \nabla \Pi_h \Phi) + (\alpha \cdot (\nabla u - \nabla u_h), \Phi - \Pi_h \Phi) - (f'(u)(u - u_h), \Phi) \\ &\quad - G(u - u_h, \Pi_h \Phi) + G(u, \Pi_h \Phi) + (f(u) - f(u_h), \Pi_h \Phi) \\ &\leq \varepsilon \|u - u_h\|_1 \|\nabla(\Phi - \Pi_h \Phi)\| + C \|\Phi - \Pi_h \Phi\| \|u - u_h\|_1 \\ &\quad - G(u - u_h, \Pi_h \Phi) + G(u, \Pi_h \Phi) - (f'(u)(u - u_h), \Phi - \Pi_h \Phi) \\ &\quad + (f(u) - f(u_h), \Pi_h \Phi) - (f'(u)(u - u_h), \Pi_h \Phi). \end{aligned}$$

By Cauchy–Schwarz inequality and the Sobolev imbedding theorem, from (8),(10) and (12), we can obtain

$$\begin{aligned} G(u - u_h, \Pi_h \Phi) &= v((I - \Pi)\nabla(u - u_h), (I - \Pi)\Pi_h \Phi) \\ &\leq v \|(I - \Pi)\nabla(u - u_h)\| \|(I - \Pi)\Pi_h \Phi\| \\ &\leq Cv h \|u - u_h\|_1 \|\Pi_h \Phi\|_1 \\ &\leq Cv h \|u - u_h\|_1 \|\Phi\|_2. \end{aligned} \tag{26}$$

$$\begin{aligned} G(u, \Pi_h \Phi) &= v((I - \Pi)\nabla u, (I - \Pi)\Pi_h \Phi) \\ &\leq v \|(I - \Pi)\nabla u\| \|(I - \Pi)\Pi_h \Phi\| \\ &\leq Cv h^2 \|u\|_2 \|\Pi_h \Phi\|_1 \\ &\leq Cv h^2 \|u\|_2 \|\Phi\|_2. \end{aligned} \tag{27}$$

From (12),(21),(22) and by Cauchy–Schwarz inequality and the Sobolev imbedding theorem, we can obtain

$$\begin{aligned} (f'(u)(u - u_h), \Phi - \Pi_h \Phi) &\leq C \|u - u_h\| \|\Phi - \Pi_h \Phi\| \\ &\leq Ch^2 \|u - u_h\| \|\Phi\|_2. \end{aligned} \tag{28}$$

$$\begin{aligned} (f(u) - f(u_h), \Pi_h \Phi) - (f'(u)(u - u_h), \Pi_h \Phi) &= (f'(u_h)(u - u_h), \Pi_h \Phi) + (f''(\phi_1)(u - u_h)^2, \Pi_h \Phi) - (f'(u)(u - u_h), \Pi_h \Phi) \\ &= ((f'(u_h) - f'(u))(u - u_h), \Pi_h \Phi) + (f''(\phi_1)(u - u_h)^2, \Pi_h \Phi) \\ &\leq C \|(u - u_h)^2\| \|\Phi\|_2. \end{aligned} \tag{29}$$

Moreover, from Sobolev imbedding inequality and (19), we can have

$$\begin{aligned} \|(u - u_h)^2\| &= \|u - u_h\|_{0,4}^2 \\ &\leq C \|u - u_h\|_1^2. \end{aligned} \tag{30}$$

From Theorem 2.1 and (24)–(30), we can obtain

$$\begin{aligned} \|u - u_h\| &\leq \frac{C}{\varepsilon} (\varepsilon h \|u - u_h\|_1 + h^2 \|u - u_h\|_1 + v h \|u - u_h\|_1 + v h^2 \|u\|_2 + \|u - u_h\|_1^2) \\ &\leq C \left(1 + \frac{v}{\varepsilon} + \frac{h}{\varepsilon}\right) h \|u - u_h\|_1 + C \frac{1}{\varepsilon} v h^2 \|u\|_2 + \frac{C}{\varepsilon} \|u - u_h\|_1^2 \\ &\leq C \left(1 + \frac{h}{\varepsilon} + \sqrt{\frac{v}{\varepsilon}}\right) \left(1 + \frac{h}{\varepsilon} + \frac{v}{\varepsilon}\right) h^2 \|u\|_2 + C \frac{1}{\varepsilon^2} \left(\varepsilon + \frac{h^2}{\varepsilon} + v\right) h^2 \|u\|_2^2. \end{aligned}$$

So we can prove the result of (20). \square

3. Two-grid method

To increase the efficiency of the algorithm, we introduce two-grid algorithm in this section. Let T_h and T_H be two quasiuniform triangulations with the mesh size h and H , respectively. Assume $h \ll H$, and the fine mesh partition T_h is generated from T_H by a mesh refinement. Then the two-grid finite element method is as follows:

Algorithm 3.1. Two-grid scheme

Step 1. Solve a nonlinear problem on the coarse mesh T_H , i.e., find $u_H \in M_H^b$ such that

$$B(u_H, v_H) + G(u_H, v_H) = (f(u_H), v_H), \quad \forall v_H \in M_H^b. \tag{31}$$

Step 2. Solve a linearized equation on a fine mesh T_h , i.e., find $u_h \in M_h^b$ to satisfy the following linear system:

$$B(u_h, v_h) + G(u_h, v_h) - (f'(u_H)u_h, v_h) = (f(u_H) - f'(u_H)u_H, v_h), \quad \forall v_h \in M_h^b. \tag{32}$$

Next, we show the error estimate of the two-grid method.

Theorem 3.1. Let $u \in H^2(\Omega) \cap H_0^1(\Omega)$ be the solution of (3), then the two-grid finite element solution u_h of (32) satisfies the following error estimate:

$$\|u - u_h\|_1 \leq C \left(\varepsilon + \frac{h}{\varepsilon} + \sqrt{\frac{\nu}{\varepsilon}} \right) h \|u\|_2 + C \frac{1}{\sqrt{\varepsilon}} \left(\varepsilon + \frac{H}{\varepsilon} + \sqrt{\frac{\nu}{\varepsilon}} \right) H^2 \|u\|_2^2. \tag{33}$$

Proof. Using Taylor expansion, we can get

$$f(u) - f(u_H) = f'(u_H)(u - u_H) + f''(\mu)(u - u_H)^2,$$

where μ is some value between u and u_H . Then subtracting Eq. (32) from Eq. (3) correspondingly, we can find that

$$B(u - u_h, v_h) + G(u - u_h, v_h) - (f'(u_H)(u - u_h), v_h) = G(u, v_h) + (f''(\mu)(u - u_H)^2, v_h). \tag{34}$$

Let $\delta = u - \Pi_h u$ and $\mu_1 = u_h - \Pi_h u$, then $u - u_h = \delta - \mu_1$. From Eq. (34), we arrive at

$$B(\delta - \mu_1, v_h) + G(\delta - \mu_1, v_h) + (f'(u_H)\mu_1, v_h) = G(u, v_h) + (f'(u_H)\delta + f''(\mu)(u - u_H)^2, v_h). \tag{35}$$

Rearranging the terms of (35), choosing $v_h = \mu_1 \in M_h^b$, we obtain:

$$\begin{aligned} & \varepsilon(\nabla \mu_1, \nabla \mu_1) + G(\mu_1, \mu_1) \\ &= \varepsilon(\nabla \delta, \nabla \mu_1) + (\alpha \cdot \nabla \delta, \mu_1) + G(\delta, \mu_1) \\ & \quad - G(u, \mu_1) - (f''(\mu)(u - u_H)^2, \mu_1) + (f'(u_H)(\mu_1 - \delta), \mu_1). \end{aligned} \tag{36}$$

Using Cauchy–Schwarz inequality and Young’s inequality and the Sobolev imbedding theorem and from (8) and (10), we have

$$\varepsilon(\nabla \delta, \nabla \mu_1) \leq \varepsilon \|\delta\|_1 \|\mu_1\|_1 \leq 4\varepsilon \|\delta\|_1^2 + \frac{\varepsilon}{16} \|\nabla \mu_1\|^2,$$

$$(\alpha \cdot \nabla \delta, \mu_1) = -(\delta, \alpha \cdot \nabla \mu_1) \leq \frac{C}{\varepsilon} \|\delta\|^2 + \frac{\varepsilon}{16} \|\nabla \mu_1\|^2,$$

$$\begin{aligned} G(\delta, \mu_1) &= \nu((I - \Pi)\nabla \delta, (I - \Pi)\nabla \mu_1) \\ &\leq \nu \|(I - \Pi)\nabla \delta\| \|(I - \Pi)\nabla \mu_1\| \\ &\leq C\nu \|\delta\|_1^2 + \frac{\nu}{4} \|(I - \Pi)\nabla \mu_1\|^2, \end{aligned}$$

$$\begin{aligned} G(u, \mu_1) &= \nu((I - \Pi)\nabla u, (I - \Pi)\nabla \mu_1) \\ &\leq \nu \|(I - \Pi)\nabla u\| \|(I - \Pi)\nabla \mu_1\| \\ &\leq C\nu h^2 \|u\|_2^2 + \frac{\nu}{4} \|(I - \Pi)\nabla \mu_1\|^2, \end{aligned}$$

$$\begin{aligned} f'(u_H)(\mu_1 - \delta, \mu_1) &= f'(u_H)((\mu_1, \mu_1) - (\delta, \mu_1)) \\ &\leq C\|\delta\| \|\mu_1\|_1 + f'(u_H)\|\nabla \mu_1\|^2 \\ &\leq \frac{\varepsilon}{16} \|\mu_1\|_1^2 + \frac{4C}{\varepsilon} \|\delta\|^2, \end{aligned}$$

$$\begin{aligned} (f''(\mu)(u - u_H)^2, \mu_1) &\leq C\|(u - u_H)^2\| \|\mu_1\|_1 \\ &\leq \frac{C}{\varepsilon} \|(u - u_H)^2\|^2 + \frac{\varepsilon}{16} \|\mu_1\|_1^2. \end{aligned}$$

From (36), we can obtain

$$\begin{aligned} &\varepsilon(\nabla\mu_1, \nabla\mu_1) + G(\mu_1, \mu_1) \\ &= \varepsilon\|\nabla\mu_1\|^2 + \nu\|(I - \Pi)\nabla\mu_1\|^2 \\ &\leq \frac{\varepsilon}{4}\|\nabla\mu_1\|^2 + \frac{\nu}{2}\|(I - \Pi)\nabla\mu_1\|^2 + C(\varepsilon + \nu)\|\delta\|_1^2 + \frac{C}{\varepsilon}\|\delta\|_0^2 + C\nu h^2\|u\|_2^2 + \frac{C}{\varepsilon}\|(u - u_H)^2\|^2. \end{aligned} \tag{37}$$

From (37), we can have

$$\varepsilon\|\nabla\mu_1\|^2 \leq C(\varepsilon + \nu)\|\delta\|_1^2 + \frac{C}{\varepsilon}\|\delta\|_0^2 + C\nu h^2\|u\|_2^2 + \frac{C}{\varepsilon}\|(u - u_H)^2\|^2. \tag{38}$$

From (14) and (38), then applying the triangle inequality, we can see that

$$\begin{aligned} &\varepsilon\|u - u_h\|_1^2 \\ &\leq 2\varepsilon(\|\delta\|_1^2 + \|\mu_1\|_1^2) \\ &\leq C(\varepsilon + \nu)\|\delta\|_1^2 + \frac{C}{\varepsilon}\|\delta\|_0^2 + C\nu h^2\|u\|_2^2 + \frac{C}{\varepsilon}\|(u - u_H)^2\|^2 \\ &\leq C\left(\varepsilon + \frac{h^2}{\varepsilon} + \nu\right)h^2\|u\|_2^2 + \frac{C}{\varepsilon}\|(u - u_H)^2\|^2. \end{aligned}$$

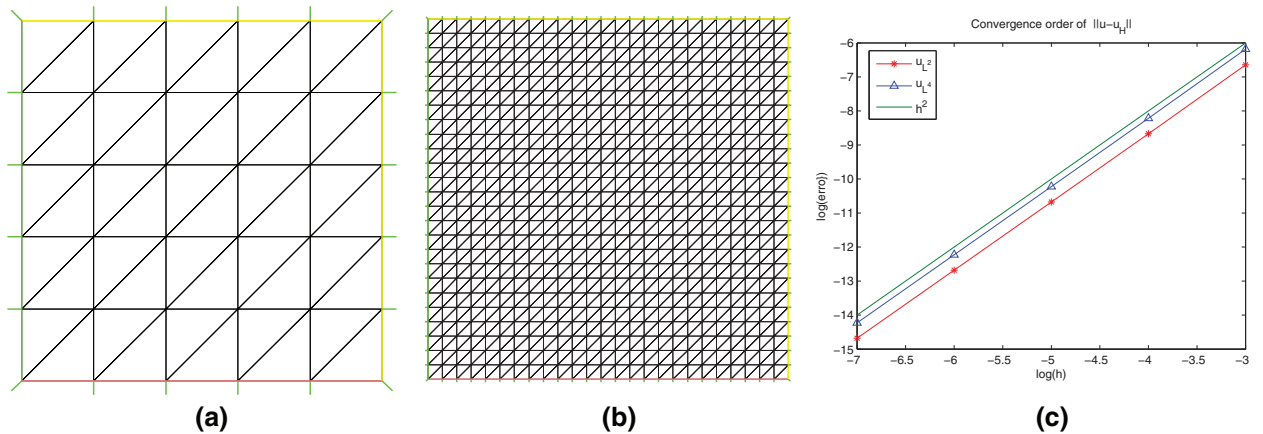


Fig. 1. (a) Coarse grid division at $H = 1/5$; (b) fine grid division at $h = 1/25$ for the two-grid method; and (c) convergence rate of u for one grid method.

Table 1
 $\varepsilon = 10^{-8}$. Relative error and convergence rate of the two-grid method.

$1/H$	$1/h$	$\frac{\ u - u_h\ }{\ u\ }$	Rate	$\frac{\ u - u_h\ _1}{\ u\ _1}$	Rate	CPU time
5	25	2.3313E-3	-	6.6102E-2	-	0.247
6	36	1.0446E-3	2.2013	4.3954E-2	1.1190	0.537
7	49	5.6387E-4	2.0001	3.2255E-2	1.0037	0.99
8	64	3.3022E-4	2.0035	2.4680E-2	1.0023	1.64
9	81	2.0618E-4	1.9993	1.9493E-2	1.0015	2.662
10	100	1.3754E-4	1.9211	1.5945E-2	0.95341	3.99
11	121	9.3681E-5	2.0148	1.3152E-2	1.0101	5.87

Table 2
 $\varepsilon = 10^{-8}$. Relative error and convergence rate of the one-grid method.

$1/h$	$\frac{\ u - u_h\ }{\ u\ }$	Rate	$\frac{\ u - u_h\ _1}{\ u\ _1}$	Rate	CPU time
25	2.1741E-3	-	6.6097E-2	-	0.53
36	9.6481E-4	2.2280	4.3953E-2	1.1189	1.217
49	5.2050E-4	2.0017	3.2257E-2	1.0035	2.23
64	3.0503E-4	2.0009	2.4682E-2	1.0022	3.793
81	1.9041E-4	2.000	1.9494E-2	1.0015	6.17
100	1.2745E-4	1.9048	1.5946E-2	0.95339	9.37
121	8.6747E-5	2.01855	1.3153E-2	1.0100	14.16

Table 3 $\varepsilon = 10^{-8}$. Relative error and convergence rate of the two-grid method with VMS.

$1/H$	$1/h$	$\frac{\ u - u_H\ }{\ u\ }$	Rate	$\frac{\ u - u_H\ _1}{\ u\ _1}$	Rate	CPU time
5	25	2.3313E-3	–	6.61026E-2	–	0.53
6	36	1.0446E-3	2.2013	4.3954E-2	1.1190	1.12
7	49	5.6387E-4	2.0001	3.2255E-2	1.0037	2.03
8	64	3.3022E-4	2.0035	2.4680E-2	1.0023	3.298
9	81	2.0618E-4	1.9993	1.9493E-2	1.0015	5.392
10	100	1.3754E-4	1.9211	1.5945E-2	0.95341	8.214
11	121	9.3681E-5	2.0148	1.3152E-2	1.0101	11.973

Furthermore, from (30), we can obtain

$$\|(u - u_H)^2\| \leq \|u - u_H\|_1^2 \leq C \frac{1}{\varepsilon} \left(\varepsilon + \frac{H^2}{\varepsilon} + \nu \right) H^2 \|u\|_2^2. \quad (39)$$

Consequently, we complete the proof of (33). \square

Remark 3.1. Theorem 3.1 shows that with two-grid scheme, the resulted solution can maintain an asymptotically optimal accuracy by taking $h = H^2$.

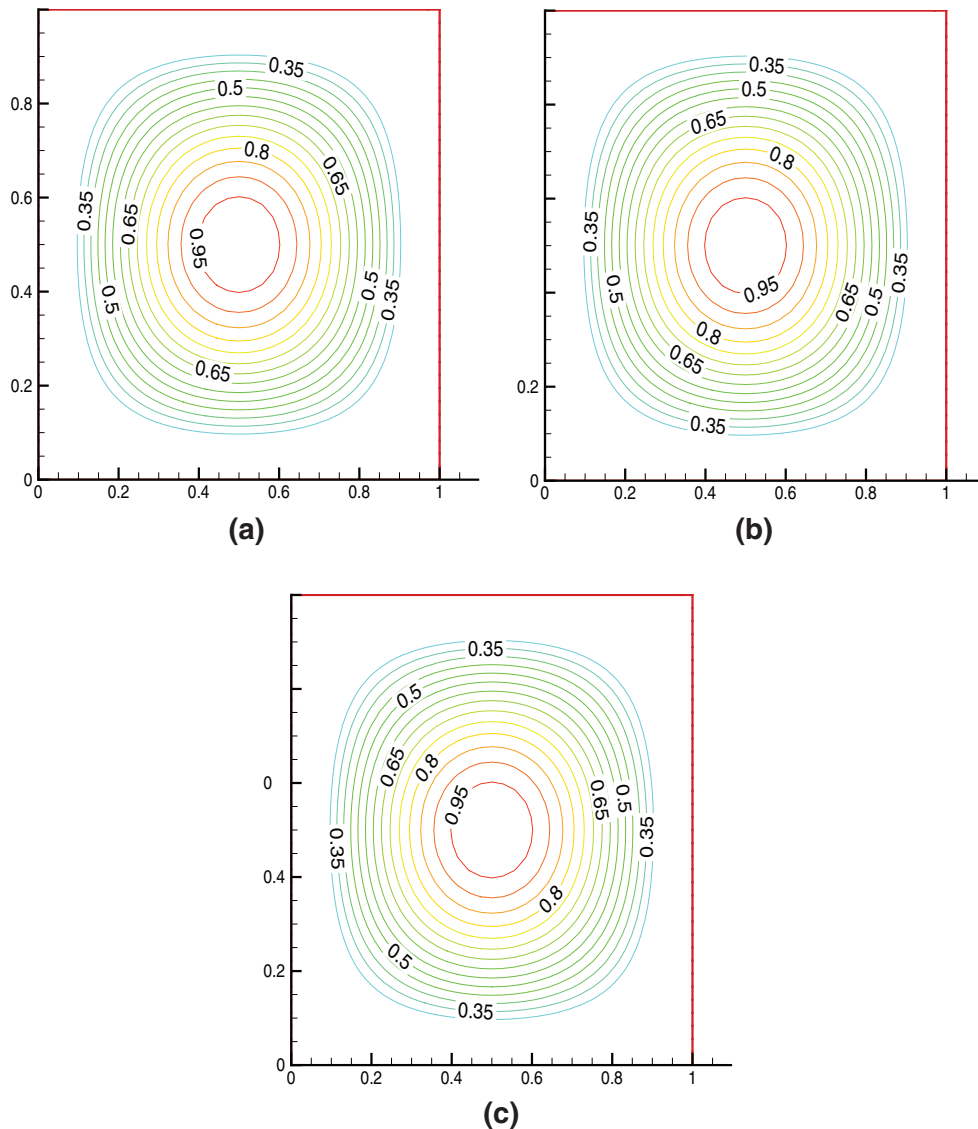


Fig. 2. (a) Numerical solution with the one grid method; (b) numerical solution with the two-grid method; and (c) numerical solution with VMS.

4. Numerical experiments

In this section we present several numerical experiments to confirm the theoretical results in the previous sections and illustrate the stability and efficiency of the two-grid locally stabilized finite element method based on local Gauss integration. The algorithms are implemented using finite element software FreeFem++ [35]. We compare our results with those obtained by the SUPG method in one grid.

In our numerical experiments, we consider the following convection–diffusion problem:

$$\alpha \cdot \nabla u - \varepsilon \Delta u + u^2 = g, \text{ in } \Omega, \quad u = 0, \text{ on } \partial\Omega. \quad (40)$$

The right-hand side $g(x, y)$ is determined by (40). In these experiments, let the computation be carried out in the region $\Omega = [0, 1] \times [0, 1]$ in R^2 . The domain Ω is uniformly divided by the triangulations of mesh size H and h in Fig. 1(a) and (b), respectively. The parameter ν is chosen as $\nu = O(h)$. To compare the two-grid method with one grid algorithm, we set $h = H^2$ in the two-grid method.

4.1. Example 1: rates of convergence study

In this experiment, the exact solution u is given as follows:

$$u = \sin(\pi x) \sin(\pi y).$$

Here we take $\varepsilon = 10^{-8}$, $\alpha = (1, \sqrt{2})$, $\nu = 0.1h$ and the right-hand side g is chosen by Eq. (40).

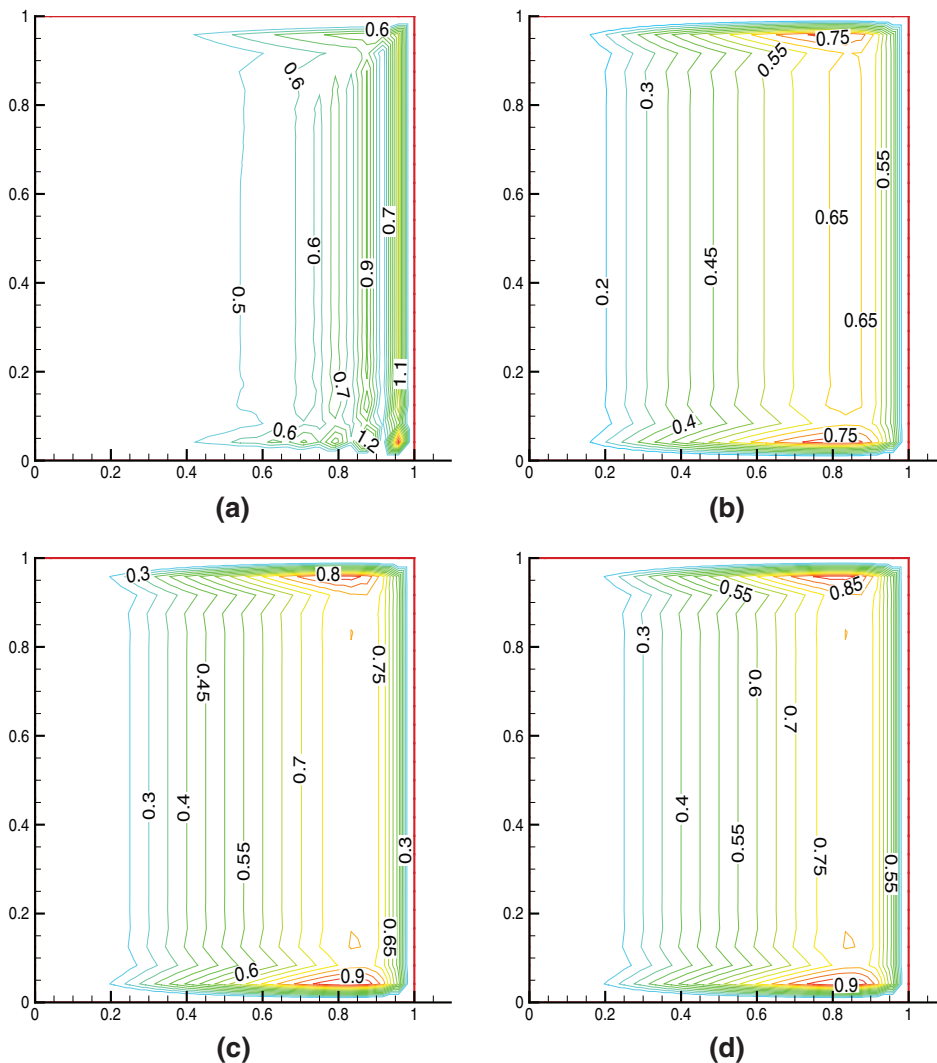


Fig. 3. (a) Numerical solution with the SUPG method; (b) numerical solution with the one grid method; (c) numerical solution with the two-grid method; and (d) numerical solution with VMS.

The CPU-time, the relative errors and the convergence rate of the two-grid method and one-grid method for different values h are tabulated in Tables 1 and 2, respectively. From Tables 1 and 2, we can find that the two-grid method and one-grid methods work well and keep the convergence rates just like the Theorem 3.1. As expected, the two-grid method takes less time than the one-grid method under nearly the same relative error. We can also compare with the common VMS method (see Eq. (7)) from [21] in Table 3. Since our method doesn't need any extra storage, compared with the common VMS method for two-grid scheme, we find that our method is less time-consuming.

Fig. 1 (c) shows the convergence order of $\|u - u_h\|$ and $\|u - u_h\|_{0,4}$ for one grid method. Moreover, we present three plots of exact and numerical solutions at the mesh $M = 36$ in Fig. 2 for the detail.

4.2. Example 2: problem with source term

To show stability and efficiency of our method, we test convection-dominated convection-diffusion problem with $\varepsilon = 10^{-9}$ and $\alpha = (1, 0)$ and $\nu = 0.01h$ and a constant source term $g = 1$. The computational domain is $\Omega = [0, 1] \times [0, 1]$, and all boundary is $u = 0$. We can find the exact solution has a 45° slope, possessing parabolic layers at $y = 0$, $y = 1$ and an exponential layer at $x = 1$ in figure.

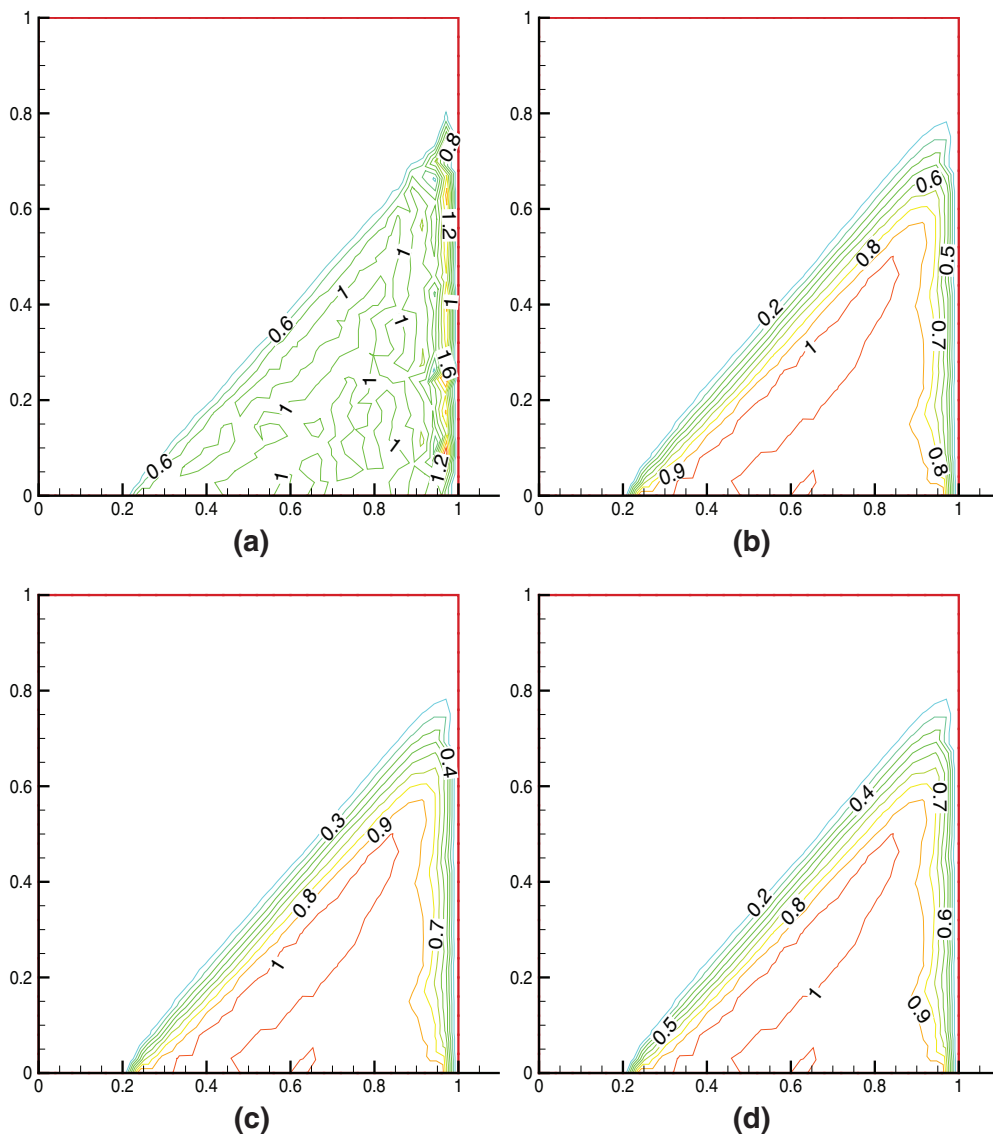


Fig. 4. (a) Numerical solution with the SUPG method; (b) numerical solution with the one grid method; (c) numerical solution with the two-grid method; and (d) numerical solution with VMS.

The solutions of the SUPG method with M_1 space is presented in Fig. 3(a). From Fig. 3, we may find that our methods have a better performance for both parabolic layers at $y = 0, y = 1$ and exponential layer at $x = 1$ than the SUPG method.

4.3. Example 3: problem with internal and external layers

Then, we consider an example which simulates a convection-dominated convection–diffusion problem with $\varepsilon = 10^{-10}$ and $\alpha = (1.0, 1.0)$ and $\nu = 0.01h$ and a constant source term $g = 0$. The computational domain is $\Omega = [0, 1] \times [0, 1]$, and all boundary is $u = 0$ at $x = 0, x = 1$ and $y = 1$; $u = 0$ at $y = 0$ if $x \leq 0.2$ and $u = 1$ if $x \leq 1$.

We can find the solution has an interior layer in the direction of the convection starting at $(0.2, 0)$ and an exponential external layer at $x = 1$. Comparing with the solution by the SUPG method (Fig. 4(a)), our method is stable near the interior layer and the exponential external layer at $x = 1$.

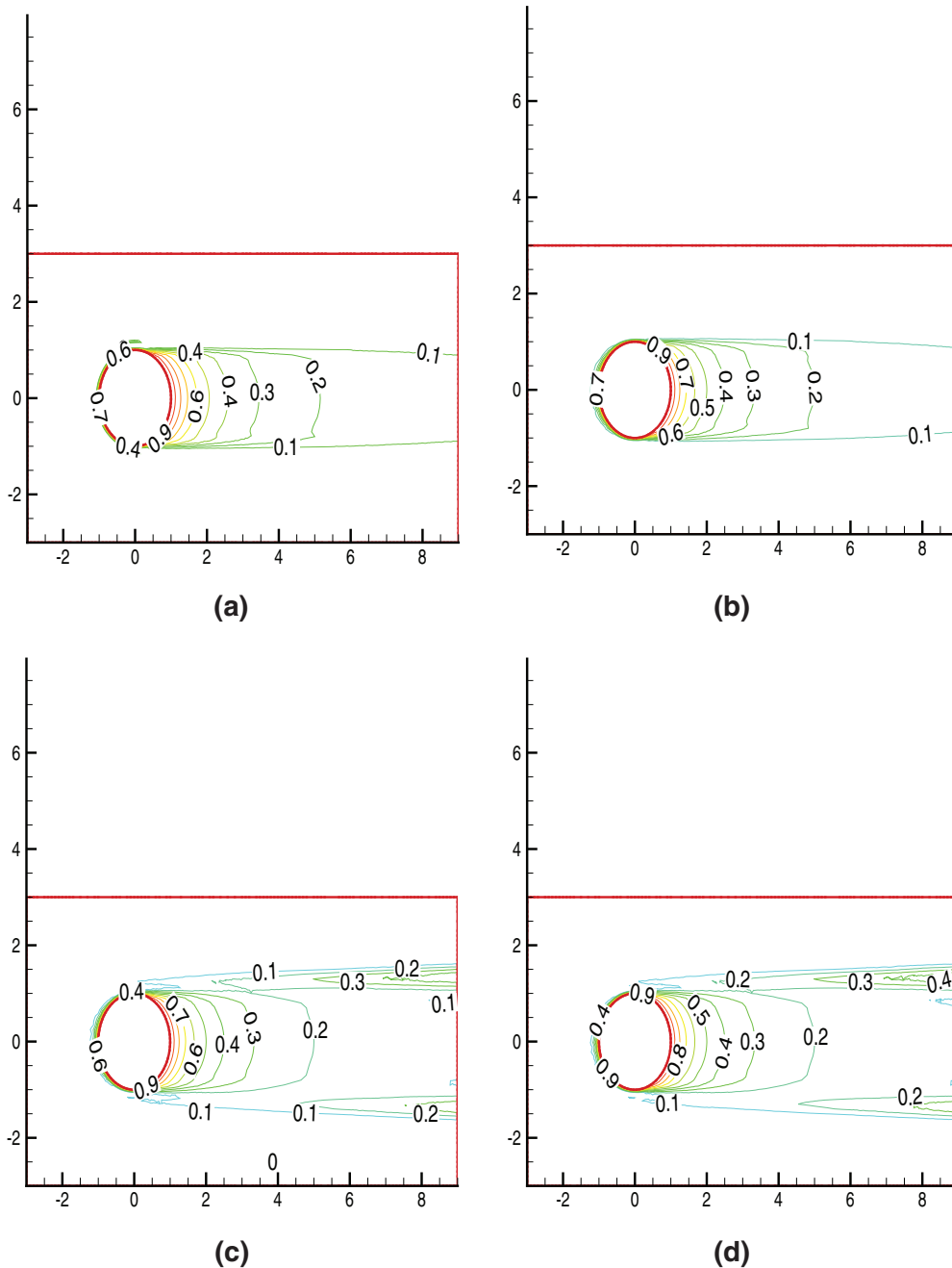


Fig. 5. (a) Numerical solution with the SUPG method; (b) numerical solution with the one grid method; (c) numerical solution with the two-grid method; and (d) numerical solution with VMS.

Table 4
CPU(s) time for the three methods.

	1/h	One grid method	Two-grid method	Common VMS method
Example 2	36	0.499	0.25	0.421
Example 3	25	0.266	0.187	0.577

4.4. Example 4: Hemker problem

Finally, we consider that the Hemker problem from [36] is a model problem for CFD, where heat transportation is along the direction of the convection in a hot column (circle) with normalized temperature $T = 1$. The problem is defined in $\Omega = \{[-3, 9] \times [-3, 3]\} \setminus \{(x, y), x^2 + y^2 \leq 1\}$, the coefficients are $\varepsilon = 10^{-8}$, $\alpha = (1.0, 0)$, $\nu = 0.01h$ and $g = 0$, and the boundary conditions are given by

$$u(x, y) = \begin{cases} 0 & \text{for } x = -3, \\ 1 & \text{for } x^2 + y^2 = 1, \\ \nu \nabla u \cdot \mathbf{n} = 0 & \text{otherwise} \end{cases} \quad (41)$$

In this problem, a boundary layer appears in the upwind direction at the circle, reaching from the bottom $(0, -1)$ to the top $(0, 1)$ of the circle. On the bottom and the top of the circle, interior layers start which spread in the direction of the convection. From Fig. 5, one can find our method provide a stable solution but the SUPG method does not.

From the above experiments, we find that one-grid, two-grid and common VMS methods present a better solution than the SUPG method. However, our two-grid method takes less CPU time compared with the other two methods, see Table 4.

5. Conclusions

In this paper, we presented a two-grid variational multiscale method based on polynomial bubble function for the convection dominated problem. The main feature of our stabilization method is that using two local Gauss integrations to replace the projection operator, which introduces no additional variables. The discussion shows that our stabilization only depends on the bubble functions. The numerical tests confirmed that our method is more efficient and reduce the computational time compared with the one-grid method and the VMS method. These ideas can be extended to the time-dependent problems and other fluid dynamical equations.

Acknowledgments

The authors would like to thank the editor and referees for their valuable comments and suggestions which helped us to improve the results of this paper. The work of J. Z. Yang is partially supported by National Science Foundation of China nos. 11171305 and 91230203, and the work of X. Lu is partially supported by National Science Foundation of China nos. 91230108 and 11471253.

References

- [1] T.J.R. Hughes, L.P. Franca, G.M. Hulbert, A new finite element formulation for computational fluid dynamics: Viii. the galerkin-least-square method for advective-diffusive equations, *Comput. Methods Appl. Mech. Eng.* 73 (1989) 173–189.
- [2] C. Baiocchi, F. Brezzi, L.P. Franca, Virtual bubbles and galerkin-least-square type methods, *Comput. Methods Appl. Mech. Eng.* 105 (1993) 125–141.
- [3] A.N. Brooks, T.J.R. Hughes, Streamline upwind petrov-galerkin formulations for convection dominated flows with particular emphasis on the incompressible navier-stokes equations, *Comput. Methods Appl. Mech. Eng.* 32 (1982) 199–259.
- [4] A. Russo, Stream-upwind petrov/galerkin method (supg) vs residual-free bubbles (rfb), *Comput. Methods Appl. Mech. Eng.* 195 (2006) 1608–1626.
- [5] F. Brezzi, A. Russo, Choosing bubbles for advection-diffusion problems, *Math. Models Methods Appl. Sci.* 4 (1994) 571–587.
- [6] L.P. Franca, A. Russo, Deriving upwinding mass lumping and selective reduced integration by residual-free bubbles, *Appl. Math. Lett.* 9 (1996) 83–88.
- [7] M. Braack, E. Burman, Local projection stabilization for the oseen problem and its interpretation as a variational multiscale method, *SIAM J. Numer. Anal.* 43 (2006) 2544–2566.
- [8] G. Matthies, P. Skrzypacz, L. Tobiska, A unified convergence analysis for local projection stabilisations applied to the oseen problem, *M2AN Math. Model. Numer. Anal.* 41 (2007) 713–742.
- [9] M. Bause, Stabilized finite element methods with shock-capturing for non-linear convection diffusion reaction models, *Numerical mathematics and advanced applications*, 2009, Springer, Berlin, Heidelberg, 2010, pp. 125–133.
- [10] M. Bause, K. Schwegler, Analysis of stabilized higher order finite element approximation of nonstationary and non-linear convection-diffusion-reaction equations, *Comput. Methods Appl. Mech. Eng.* 209 (2012) 184–196.
- [11] M. Bause, K. Schwegler, Higher order finite element approximation of systems of convection diffusion reaction equations with small diffusion, *J. Comput. Appl. Math.* 246 (2013) 52–64.
- [12] H. Yücel, M. Stoll, P. Benner, Discontinuous galerkin finite element methods with shock capturing for non-linear convection dominated models, *Comput. Chem. Eng.* 58 (2013) 278–287.
- [13] T.J.R. Hughes, Multiscale phenomena: greens functions, the dirichlet-to-neumann formulation, subgrid-scale models, bubbles and the origins of stabilized methods, *Comput. Methods Appl. Mech. Eng.* 127 (1995) 387–401.
- [14] T. Hughes, L. Mazzei, K. Jansen, Large eddy simulation and the variational multiscale method, *Comput. Vis. Sci.* 3 (2000) 47–59.
- [15] T.J.R. Hughes, L. Mazzei, A.A. Oberai, The multiscale formulation of large eddy simulation: decay of homogeneous isotropic turbulence, *Phys. Fluids* 13 (2001) 505–511.

- [16] J.-L. Guermond, Stabilization of galerkin approximations of transport equations by subgrid modeling, *M2AN Math. Model. Numer. Anal.* 33 (1999) 1293–1316.
- [17] W. Layton, A connection between subgrid scale eddy viscosity and mixed methods, *Appl. Math. Comput.* 133 (2002) 147–157.
- [18] S. Kaya, W. layton, B. Riviere, Subgrid stabilized defect correction methods for the navier-stokes equations, *SIAM Numer. Anal.* 44 (2006) 1639–1654.
- [19] H.B. Zheng, Y.R. Hou, F. Shi, Adaptive variational multiscale methods for incompressible flows based on two local gauss integrations, *J. Comput. Phys.* 229 (2010) 7030–7041.
- [20] L.N. Song, Y.R. Hou, H.B. Zheng, A variational multiscale method based on bubble functions for convection-dominated convection-diffusion equation, *Appl. Math. Comput.* 217 (2010) 2226–2237.
- [21] V. John, S. Kaya, W. Layton, A two-level variational multiscale method for convection-dominated convection-diffusion equations, *Comput. Methods Appl. Mech. Eng.* 195 (2006) 4594–4603.
- [22] J. Xu, A novel two-grid method for semilinear elliptic equations, *SIAM J. Sci. Comput.* 15 (1994) 231–237.
- [23] J. Xu, Two-grid finite element discretization techniques for linear and nonlinear pde, *SIAM J. Numer. Anal.* 33 (1996) 1759–1777.
- [24] L. Chen, Y. Chen, Two-grid method for nonlinear reaction-diffusion equations by mixed finite element methods, *J. Sci. Comput.* 49 (2011) 383–401.
- [25] Y. He, A. Wang, A simplified two-level method for the steady navier-stokes equations, *Comput. Methods Appl. Mech. Engrg.* 197 (2008) 1568–1576.
- [26] Y.N. He, K.T. Li, Two-level stabilized finite element methods for the steady navier-stokes problem, *Computing* 74 (2005) 337–351.
- [27] Y.N. He, Y. Zhang, H. Xu, Two-level newton's method for nonlinear elliptic pdes, *J. Sci. Comput.* 57 (2013) 124–145.
- [28] Y. Zhang, Y. He, A two-level finite element method for the stationary navier-stokes equations based on a stabilized local projection, *Numer. Methods Partial Differ. Equ.* 27 (2011) 460–477.
- [29] Y.Q. Shang, A parallel two-level linearization method for incompressible flow problems, *Appl. Math. Lett.* 24 (2011) 364–369.
- [30] P. Huang, X. Feng, D. Liu, Two-level stabilized method based on three corrections for the stationary navier-stokes equations, *Appl. Numer. Math.* 62 (8) (2012) 988–1001.
- [31] Z. Weng, Z. Yang, X. Lu, Two level quadratic equal-order stabilized method for the stokes eigenvalue problem, *Int. J. Comput. Math.* 92 (2015) 337–348.
- [32] P. Bochev, C.R. Dohrmann, M.D. Gunzburger, Stabilization of low-order mixed finite elements for the stokes equations, *SIAM J. Numer. Anal.* 44 (2006) 82–101.
- [33] E. Burman, P. Hansbo, Edge stabilization for galerkin approximations of convection–diffusion reaction problems, *Comput. Method. Appl. Mech. Eng.* 193 (2004) 1437–1453.
- [34] V. Girault, P.-A. Raviart, *Finite Element Methods for the Navier-Stokes Equations: Theory and Algorithms*, Springer, Berlin, 1986.
- [35] F. Hecht, New development in freefem++, *J. Numer. Math.* 20 (3–4) (2012) 251–265.
- [36] M. Auguston, A. Caiazzo, A. Fiebach, J. Fuhrmann, V. John, A. Linke, R. Umla, An assessment of discretizations for convection-dominated convection-diffusion equations, *Comput. Methods Appl. Eng.* 200 (2011) 3395–3409.